Assignment 3

Digital Signal Processing

AE4463P-23: Advanced Aircraft Noise

E. Oosthoek, J. Bogaert

Delft University of Technology

TU Delft

Assignment 3

Digital Signal Processing

by

E. Oosthoek, J. Bogaert

Student Name	Student Number
Elisabeth Oosthoek	5056470
Joshua Bogaert	5298601

Instructors: Prof. dr. ir. M. Snellen, Prof. dr. D.G. Simons
Faculty: Faculty of Aerospace Engineering, Delft

Cover: https://unsplash.com/photos/white-and-blue-airplane-under-white-clouds-during-daytime-bNVbyBl870A
Style: TU Delft Report Style, with modifications by Daan Zwaneveld

TU Delft

1 ANOPP Model

Within this report a semi-empirical method developed by NASA will be utilised to estimate and analyse the noise being produced by various aircraft components. The above mentioned method developed by NASA called ANOPP (short for NASA's Aircraft Noise Prediction Program) was exclusively used within this report, however the formulations summarised within [1] were used to create the code model (which can be reviewed in chapter 2).

Utilising the ANOPP, the noise created due to four air-frame components will be analysed. These components include the main landing gear, leading edge flaps, trailing edge slats and clean wing of the *B737*. It must be noted that, although these components are significant contributor's to the noise being generated by the aircraft, there still are a range of other contributors such as the engine and tail.

1.1. Modeling noise due to singular components

The main purpose of the code was to estimate the "p-squared" term, or effective pressure squared. This evaluation of the effective pressure was done for the first 43 one-third octave band central frequencies. To estimate the effective pressure term Equation 1.1 was utilised, while for the one-third octave bands Equation 1.2 was utilised. Both expression were extracted from [1]

$$p_e^2\left(f,\theta,\phi\right) = \frac{\rho_\infty c P D(\theta,\phi) F(s)}{4\pi r^2 (1 - M\cos\theta)^4} \tag{1.1}$$

$$f_n = 10^{\frac{n}{10}} \quad \text{with n being the band number (1 to 43)} \tag{1.2}$$

For each of the aforementioned air-frame components the effective pressure squared was then determined for the various frequencies. It must be mentioned that the terms (P, F, D), as found in Equation 1.1 are dependent on the component being analysed. Here P is the power function, F is the spectral function which relies on the Strouhal number as input and D is the directivity function. The exact formulation can be reviewed in chapter 2 and [1]. Furthermore the following values were assumed $\theta = \pi/2$, $\phi = 0$ (aircraft is located overhead, resulting in mentioned θ and ϕ), $r = 1$, $\delta_f = \pi/6$, $\mu = 1.84 * 10^{-5} \frac{kg}{m*s}$, $\rho = 1.225 \frac{kg}{m^3}$ and $c = 340.3\,\mathrm{m\,s^{-1}}$.

Now utilising the determined values in pascal squared and relating them to power spectral density values expressed in db/Hz, while also correcting for the one-third octave bands, the following results were obtained as seen in Figure 1.1.

The equation below was utilised to compute the corrected power spectral density as a function of the one-third octave band central frequencies for individual components.

$$PSD_n = 10\log_{10}\left(\frac{(p_e^2)_n / f_n}{p_{e,0}^2}\right) - 10\log_{10}\left(0.23 * f_n\right) \quad \left[\frac{dB}{Hz}\right] \tag{1.3}$$

To compute the total power spectral density the above relation can still be utilised. However now first the individual effective pressure squared terms for the various components are summed together. This new term is then utilised instead of previous effective pressure squared term. As result using Equation 1.3 the total power spectral density as a function of the various frequencies is found.

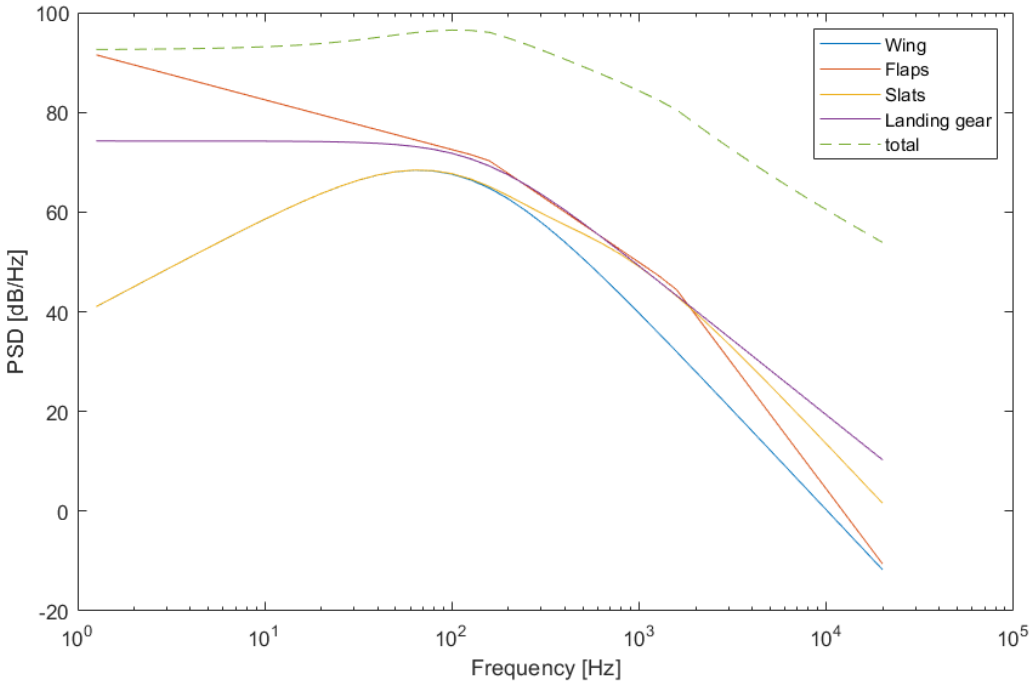

Figure 1.1: The power spectral density as a function of frequency resulting from the ANOPP model. The results are resented on component and full level.

Within Figure 1.1 the contributions of the various individual components can be observed, as can the sum of the four elements. Firstly it can be observed that when observing the total contribution large power spectral density values (PSD) are observed for the lower frequencies (up to 200 Hz), where after the levels drastically drop for the higher frequencies (from 200Hz to 20000Hz). Therefore it can be seen that from the ANOPP model, it can be evaluated that air-frame noise is mainly concentrated within the ”lower” frequencies. Within the section 1.2 this evaluation will be compared to measurements to evaluate if the model represents reality.

For the individual components it can be noticed that the wing and slats follow a similar behaviour. Both initially have a PSD of 40 dB/Hz, reach a maximum of 68 dB/hz at 63Hz. Following this maximum the values quickly decrease in magnitude. This last behaviour can be noticed for all four components analysed. From the model it can therefore be mentioned that the slats and the wing both produced broadband noise, however a strong tonal contribution can be observed.

For the main landing gear and the slats the highest contribution is observed in the lower frequencies (up to $\pm$ 100Hz). However the Flaps the initial value is higher (92dB), followed by a negative slope. Whereas the main landing gear stays constant at 74 decibels during this low frequency phase. Afterwards both follow the global downwards trend.

1.2. Comparison between modeled and measured results

A model, when implemented correctly will always produce an output. However it is vital to compare the model output with data to investigate if the model represents reality to an acceptable level. A set of measurements

were provided for the B737 aircraft flying overhead. Here the power spectral density were provided for the equivalent one-third octave bands central frequencies as presented previously. Superimposing the modeled data with the measured data the following is observed.

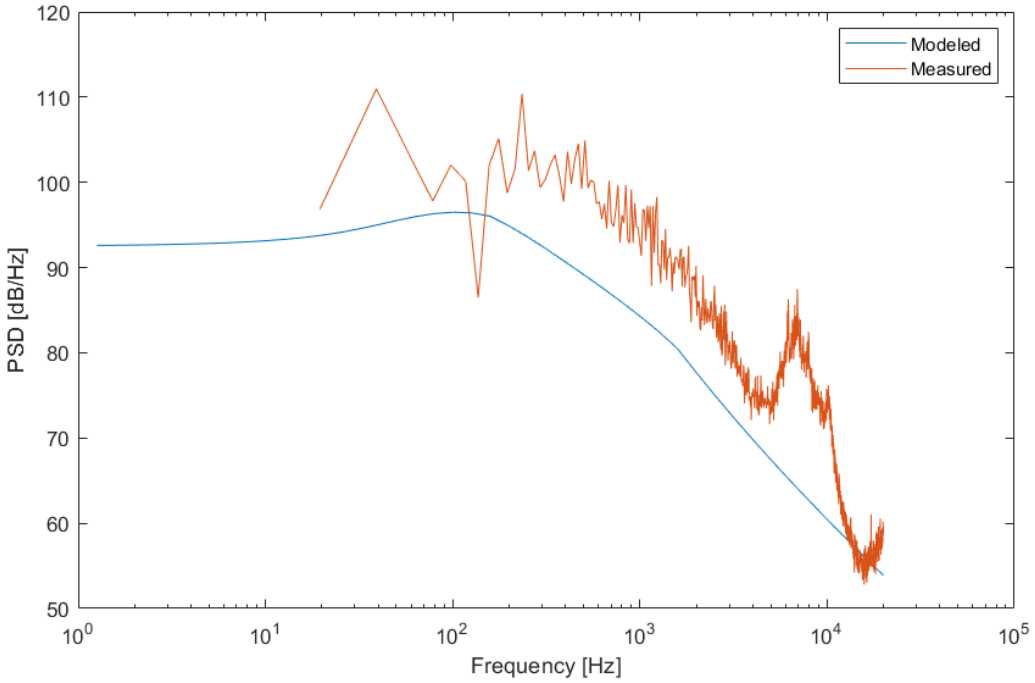

Figure 1.2: Modeled PSD as a function of frequency compared to measured values

When performing a comparison between the measured and modelled data a range of observations can be made. Firstly it can be seen that for the full frequency spectrum the modelled results under estimate reality (measured PSD levels). This behaviour can be explained by a few considerations. First, the ANOPP model utilised here does not take into account contributions due to the nose landing gear, the fuselage, tail and engine (as mentioned in [1], the engine noise can be a complex phenomenon to model, especially when insufficient data is available). All of the above mentioned components are also significant contributors to the sound levels, and therefore could be a first reasoning behind the lower values. Secondly, within the modelled data the aircraft was assumed to be exactly overhead at a distance of 1 meter, these could be slightly different then reality. Lastly, the ANOPP method, as explained previously is a semi-empirical method, it relies on physics and data measurements for its results. These methods aim to provide good solutions for a wide range of scenarios, however of course are not able to predict the exact situation the actual measurements were performed in (atmosphere, temperature, weather, humidity, density). This last points also link nicely to the values which were assumed within the report, since these may also deviate from the values which were utilised the day the measurements were performed.

Other observations that can be made are that the overall shape of both data sources show strong similarity. Meaning that the modelled results do correctly predict the strong contribution of the air-frame to the lower frequencies. This strong contribution is then followed by a strong decline. The peak which can be observed within the measured data near the 6000 to 7000Hz frequencies, is due to the noise being generated by the engine. The engine (fan) produces noise at a much higher frequency when compared to the air-frame. Which explains the quick rise (tonal noise) towards the higher frequencies. Furthermore data which is measured, is almost always characterised by noise which can also be evaluated within the figure.

A second comparison which can be performed between the measured and modeled data, is trough a comparison of overall sound pressure level values (OSPL). Trough this comparison the intensity of the event, can be analysed, taking into account the full frequency spectrum. The following relation is used, utilising

Equation 1.4 the data presented in Figure 1.2.

$$OPSL = 10 * log_{10}\left(\sum_{n} 10^{PSD_n/10}\right) \quad [dB] \tag{1.4}$$

For the measured data the overall sound pressure level was computed to be 119.316 dB. While for the modelled data this OSPL value was 108.437 dB, approximately 10 % lower in comparison to the measured results. This can be explained due to reasoning provided previously for the underestimations.

To conclude, through the implementation of the ANOPP method it is possible to model aircraft noise being generated by a range of air-frame components. Although the estimated values do underestimate reality, they do provide good first estimates into the relative importance of various components to the overall noise levels. Furthermore the model provides flexibility to very quickly test a range of combinations, making the analysis of a range of options quickly feasible.

References

[1] Prof. dr. ir. M. Snellen Prof. dr. D.G. Simons. *An introduction to general acoustics and aircraft noise*. 1th ed. Delft, Netherlands: TU Delft, 2023.

2
Matlab code

```
%% Assignment 3: Advanced Aircraft Noise
% By: Elisabeth and Joshua

clear;

% tdfread('data_asignment3','\t')
data = importdata('data_asignment3');

%%% Start Script %%%

%% Aircraft Data (737)

v = 81; % m/s
A_w = 130; % m^2
b_w = 34; % m
A_f = 18; % m^2
b_f = 17; % m
d = 1.1; % m
n_w = 2;
n_b = 2;
n = n_w*n_b;

mu = 1.84*10^(-5); % kg/(m*s)
rho = 1.225;
c = 340.3;

M = v/c;

band_numbers = 1:1:43;
f = 10.^(band_numbers/10);

% assumed values
theta = pi / 2;
phi = 0;
r = 1;
delta_f = pi/6;

%% Formulas lg

K = 3.414*10^(-4);
a = 6;
G = n*(d/b_w)^2;
L = d;

% Power function
P = K*(M^a)*G*rho*(c^3)*(b_w^2);

% Strouhal number
S = (f * L * (1 - M*cos(theta))) / (M*c);

% Spectral function
F = 0.0577 .* (S.^2) .* ((0.25*S.^2) + 1).^(-1.5);

%figure();
%loglog(S,F)
%hold on
```

```
57
58 % Directivity funtion
59 D = (3/2)*(sin(theta))^2;
60
61 %
62 psquared_lg = (rho*c*P*D*F) / (4*(pi^2)*(r^2)*(1-M*cos(theta))^4);
63
64 %% Flaps formulas
65 K = 2.787*10^(-4);
66 a = 6;
67 G = (A_f/(b_w^2))*(sin(delta_f))^2;
68 L = A_f/b_f;
69
70 % Power function
71 P = K*(M^a)*G*rho*(c^3)*(b_w^2);
72
73 % Strouhal number
74 S = (f * L * (1 - M*cos(theta))) / (M*c);
75
76 % Spectral function
77 F = zeros(size(S));
78
79 % Apply the conditions for each range
80 F(S < 2) = 0.0480 * S(S < 2);
81 F((2 <= S) & (S <= 20)) = 0.1406 * S((2 <= S) & (S <= 20)).^(-0.55);
82 F(S > 20) = 216.49 * S(S > 20).^(-3);
83
84 %loglog(S,F)
85
86 % Directivity funtion
87 D = 3*(sin(delta_f)*cos(theta)+cos(delta_f)*sin(theta)*cos(phi))^2;
88
89 psquared_fl = (rho*c*P*D*F) / (4*(pi^2)*(r^2)*(1-M*cos(theta))^4);
90
91 %% Formulas (wing)
92 K = 4.464*10^(-5);
93 a = 5;
94 G = 0.37*(A_w / b_w^2)*((rho*M*c*A_w) / (mu*b_w))^(-0.2);
95 L = G*b_w;
96
97 % Power function
98 P = K*(M^a)*G*rho*(c^3)*(b_w^2);
99
100 % Strouhal number
101 S = (f * L * (1 - M*cos(theta))) / (M*c);
102
103 % Spectral function
104 F = 0.613 * ((10*S).^4) .* (((10*S).^(1.5)) + 0.5).^(-4);
105
106 %loglog(S,F)
107
108 % Directivity funtion
109 D = 4 * (cos(phi)^2) * (cos(theta / 2)^2);
110
111 %
112 psquared_wg = (rho*c*P*D*F) / (4*(pi^2)*(r^2)*(1-M*cos(theta))^4);
113
114 %% Formulas (slats)
115
116 K = 4.464*10^(-5);
117 a = 5;
118 G = 0.37*(A_w / b_w^2)*((rho*M*c*A_w) / (mu*b_w))^(-0.2);
119 L = G*b_w;
120
121 % Power function
122 P = K*(M^a)*G*rho*(c^3)*(b_w^2);
123
124 % Strouhal number
125 S = (f * L * (1 - M*cos(theta))) / (M*c);
126
127 % Spectral function
```

```
F = (0.613 * ((10*S).^4) .* (((10*S).^(1.5)) + 0.5).^(-4)) ...
    + (0.613 * ((2.19*S).^(4)) .* (((2.19*S).^1.5) + 0.5).^(-4));

% loglog(S,F)

% Directivity funtion
D = 4 * (cos(phi)^2) * (cos(theta / 2)^2);

%
psquared_sl = (rho*c*P*D*F) / (4*(pi^2)*(r^2)*(1-M*cos(theta))^4);

%% Plots

figure();
semilogx(data(1,:), data(2,:))

res_wg = 10*log10((psquared_wg ./ f) / (2*10^(-5))^2);
res_fl = 10*log10((psquared_fl ./ f) / (2*10^(-5))^2);
res_sl = 10*log10((psquared_sl ./ f) / (2*10^(-5))^2);
res_lg = 10*log10((psquared_lg ./ f) / (2*10^(-5))^2);

res_wg = res_wg - 10*log10(0.23*f);
res_fl = res_fl - 10*log10(0.23*f);
res_sl = res_sl - 10*log10(0.23*f);
res_lg = res_lg - 10*log10(0.23*f);

semi = 10 * log10((psquared_wg + psquared_fl + psquared_sl + psquared_lg ) / (2*10^(-5))^2 );
res_tot = semi - 10*log10(0.23*f);

figure();
semilogx(f, res_wg)
hold on
semilogx(f, res_fl)
semilogx(f, res_sl)
semilogx(f, res_lg)
semilogx(f, res_tot, LineStyle="--")
legend("Wing", "Flaps", "Slats", "Landing gear", "total")
xlabel('Frequency␣[Hz]')
ylabel('PSD␣[dB/Hz]')

%% Comparison measured and modelled

figure();
semilogx(f,res_tot)
hold on
semilogx(data(1,:), data(2,:))
legend("Modeled", "Measured")
xlabel('Frequency␣[Hz]')
ylabel('PSD␣[dB/Hz]')

%% OSPL for both measure and modeled sound data

OSPL_mdl = 10*log10(sum(10.^(res_tot/10)));
OSPL_msr = 10*log10(sum(10.^(data(2,:)/10)));
```